

LGN Input to Simple Cells and Contrast-Invariant Orientation Tuning: An Analysis

TODD W. TROYER,¹ ANTON E. KRUKOWSKI,² AND KENNETH D. MILLER³

¹Department of Psychology, Neuroscience and Cognitive Science Program, University of Maryland, College Park, Maryland 20742; ²National Aeronautics and Space Administration Ames Research Center, Moffett Field 94035-1000; and ³Departments of Physiology and Otolaryngology, W. M. Keck Center for Integrative Neuroscience, Sloan-Swartz Center for Theoretical Neurobiology, University of California, San Francisco, California 94143-0444

Received 8 June 2001; accepted in final form 12 February 2002

Troyer, Todd W., Anton E. Krukowski, and Kenneth D. Miller. LGN input to simple cells and contrast-invariant orientation tuning: an analysis. *J Neurophysiol* 87: 2741–2752, 2002; 10.1152/jn.00474.2001. We develop a new analysis of the lateral geniculate nucleus (LGN) input to a cortical simple cell, demonstrating that this input is the sum of two terms, a linear term and a nonlinear term. In response to a drifting grating, the linear term represents the temporal modulation of input, and the nonlinear term represents the mean input. The nonlinear term, which grows with stimulus contrast, has been neglected in many previous models of simple cell response. We then analyze two scenarios by which contrast-invariance of orientation tuning may arise. In the first scenario, at larger contrasts, the nonlinear part of the LGN input, in combination with strong push-pull inhibition, counteracts the nonlinear effects of cortical spike threshold, giving the result that orientation tuning scales with contrast. In the second scenario, at low contrasts, the nonlinear component of LGN input is negligible, and noise smooths the nonlinearity of spike threshold so that the input-output function approximates a power-law function. These scenarios can be combined to yield contrast-invariant tuning over the full range of stimulus contrast. The model clarifies the contribution of LGN nonlinearities to the orientation tuning of simple cells and demonstrates how these nonlinearities may impact different models of contrast-invariant tuning.

INTRODUCTION

The tuning of visual neurons for the orientation of contrast edges is the most thoroughly explored response property of cortical neurons. Cortical layer 4 of cat primary visual cortex (V1) is composed primarily of simple cells (Bullier and Henry 1979; Gilbert 1977; Hubel and Wiesel 1962), i.e., cells with receptive fields (RFs) containing oriented subregions each responding exclusively to either light onset/dark offset (ON subregions) or dark onset/light offset (OFF subregions). Hubel and Wiesel (1962) proposed that these response properties arose from a corresponding, oriented arrangement of inputs to simple cells from ON-center and OFF-center cells in the lateral geniculate nucleus (LGN) of the thalamus; such an arrangement is referred to as Hubel-Wiesel thalamocortical connectivity. The usual formulation of this so-called “feed-forward” model assumes that simple cell response properties arise from a linear summation of these LGN inputs, followed by a rectification nonlinearity due to spike

threshold (Carandini and Ferster 2000; Ferster 1987; Ferster and Miller 2000).

The feed-forward model is challenged by the fact that spiking responses in simple cells are invariant to changes in stimulus contrast (Sclar and Freeman 1982; Skottun et al. 1987): under this model, inputs at nonoptimal orientations are expected to be subthreshold at low contrast but become supra-threshold at higher contrast. We have previously presented simulation results showing that a simple form of strong “push-pull” inhibition (inhibition induced by light in OFF subregions or dark in ON subregions), combined with Hubel-Wiesel thalamocortical connectivity, is sufficient to overcome this difficulty and robustly yield contrast-invariant orientation tuning (Troyer et al. 1998). In this paper, we analyze the conditions required to achieve contrast-invariant orientation tuning in such a push-pull model.

In our previous work, we studied two versions of the push-pull model. In one version (“network model”), the cortex was modeled as a fairly realistic network of spiking neurons, each modeled as a single-compartment conductance-based integrate-and-fire neuron. The LGN responses were modeled as Poisson spike trains sampled from the stimulus-driven LGN firing rates. The second version (“conceptual model”) was much simpler. In this model, both cortical and LGN neuronal activities were represented by firing rates, and the only nonlinearity was the rectification of firing rates at some threshold level of input (rates could not go below zero). While the network model also included intracortical connections from excitatory neurons, the conceptual model included only direct thalamic excitation and thalamic-driven feed-forward inhibition (meaning inhibition driven by LGN via inhibitory cortical interneurons).¹ Despite the differences, the two models pro-

¹ By referring to feed-forward inhibition, we refer to that component of the inhibition driven by the LGN. A single inhibitory cell might be driven both by LGN and by cortical cells, so that it could contribute both feed-forward and feedback inhibition. In Troyer et al. (1998) we showed that the feed-forward component of the inhibition was necessary and sufficient to yield contrast-invariant tuning, and that the feedback component had no effect on orientation tuning in the context of the model circuit studied there.

The costs of publication of this article were defrayed in part by the payment of page charges. The article must therefore be hereby marked “advertisement” in accordance with 18 U.S.C. Section 1734 solely to indicate this fact.

Address for reprint requests: T. W. Troyer, Dept. of Psychology, University of Maryland, College Park, MD 20742 (E-mail: ttroyer@glue.umd.edu).

duced quantitatively similar orientation tuning curves.² This suggests that the simpler conceptual model retained the key elements responsible for contrast-invariant orientation tuning in the more complex model, and in particular that the rectification or threshold nonlinearity is the primary nonlinearity that is essential for an understanding of this tuning.

In this article, we characterize the conditions required for contrast invariance in the conceptual model, which is simple enough to allow analysis. We begin by deriving a general equation for the total LGN input to a cortical simple cell receiving Hubel-Wiesel thalamocortical connections, making minimal assumptions other than that LGN responses can be well-described by an instantaneous firing rate and that the total LGN input to the simple cell is given by an appropriately weighted sum of the LGN firing rates. We then show that, in the case of a periodic grating stimulus, this equation is dominated by two terms: a linear term, representing the sinusoidally modulated part of the input, and a nonlinear term, representing the mean input. Except at very low stimulus contrasts, this nonlinear term grows with stimulus contrast due to the rectification of LGN firing rates. We then examine how the combination of this LGN input, LGN-driven push-pull inhibition, and a cortical cell threshold can yield contrast-invariant orientation tuning in two regimes. In one regime, representing all but very low contrasts, contrast invariance of orientation tuning can arise if the growth of the linear and the nonlinear input terms have the same shape as a function of contrast. Further analysis demonstrates that this condition should be at least approximately true for a wide range of LGN models. In the second regime, representing very low contrasts, the nonlinear input term does not change with contrast, so that the stimulus-induced input is simply given by the linear term, which scales with contrast. In this regime, where the total input is small, input noise results in a smoothed threshold. Over a wide range of thresholds, this smoothing results in an input/output function that is approximated by a power-law function (Miller and Troyer 2002). The combination of input that scales with contrast and a power-law input/output function yields contrast-invariance of tuning. Finally, we demonstrate that these two mechanisms can combine to yield contrast-invariant tuning over all contrasts.

An abstract of this work has appeared (Troyer et al. 1999).

RESULTS

LGN input to simple cells

Previous investigations into the origins of orientation selectivity have made a variety of simplifying assumptions regarding the nature of the LGN input to cortical simple cells. Often, the visual stimulus is transformed directly into a pattern of cortical input, ignoring important nonlinearities contributed by LGN responses. In this paper we focus on periodic gratings, i.e., stimuli that are spatially periodic in one dimension and uniform in the other dimension. Our model is a purely spatial model and ignores cortical temporal integration. We consider

² The two models differed at the lowest contrast studied, 2.5%, where the network model but not the conceptual model maintained contrast-invariant tuning. This difference arose because noise was present in the network model but not in the conceptual model; adding noise to the conceptual model eliminates this difference, see RESULTS.

an “instantaneous” pattern of LGN activity across a sheet of cells indexed by the two dimensional vector \mathbf{x} representing the center of each LGN receptive field. Cortical output is derived as a static function of this pattern of activity.

In this section, we demonstrate that the total LGN input to a simple cell in response to a grating stimulus with contrast C , orientation θ , and spatial location given as a phase variable ϕ_{stim} , can be well approximated by a function of the following form

$$I_{\text{LGN}}(C, \theta, \phi_{\text{stim}}) \cong \text{DC}(C) + \text{F1}_{\text{max}}(C)h(\theta) \cos(\phi_{\text{stim}}) \quad (1)$$

Equation 1 will be derived using a series of arguments demonstrating, in sequential subsections, that

1) I_{LGN} can be written as a sum of two terms. One term corresponds to a linear response model and represents input that is reversed in sign if the sign of the receptive field is reversed. The second term represents a nonlinear response to the stimulus and is unchanged by an overall sign reversal of the receptive field.

2) For periodic grating stimuli, the second term represents the mean (DC) level of input averaged over all spatial phases, while the first term represents a sinusoidal (1st harmonic or F1) modulation of the input as a function of the grating’s spatial phase.

3) The level of the mean input depends only on contrast. The amplitude of the modulation can be factored into the product of a function that depends only on contrast and a function that depends only on orientation.

Input from a Gabor RF: general expression

We view the LGN as a uniform sheet of ON-center and OFF-center X cells, and let $L^{\text{ON}}(\mathbf{x})$ [$L^{\text{OFF}}(\mathbf{x})$] denote the response of the LGN ON (OFF) cell at position vector \mathbf{x} at a particular time t [for simplicity, we omit the time dependence in $L^{\text{ON}}(\mathbf{x}, t)$ and $L^{\text{OFF}}(\mathbf{x}, t)$]. Initially, we make no explicit assumptions regarding the relationship between ON and OFF cells responses. However, we expect ON and OFF cells at the same location to have roughly opposite responses to changes in luminance. To extract the ON/OFF difference we let $L^{\text{diff}}(\mathbf{x}) = [L^{\text{ON}}(\mathbf{x}) - L^{\text{OFF}}(\mathbf{x})]/2$. Letting $L^{\text{avg}}(\mathbf{x}) = [L^{\text{ON}}(\mathbf{x}) + L^{\text{OFF}}(\mathbf{x})]/2$ denote the average LGN response at position \mathbf{x} , we can rewrite $L^{\text{ON}}(\mathbf{x}) = L^{\text{avg}}(\mathbf{x}) + L^{\text{diff}}(\mathbf{x})$ and $L^{\text{OFF}}(\mathbf{x}) = L^{\text{avg}}(\mathbf{x}) - L^{\text{diff}}(\mathbf{x})$.

We assume that the spatial pattern of LGN connections to a simple cell can be described by a Gabor function (Jones and Palmer 1987b; Reid and Alonso 1995). For simplicity, we will refer to this pattern of LGN connectivity as the receptive field (RF) of the cell. We let the vector \mathbf{f}^{RF} represent the preferred spatial frequency and orientation of the RF, and choose our \mathbf{x} coordinates so that \mathbf{f}^{RF} is parallel to the x_1 axis and so that the RF center is at the origin. Thus we write the Gabor RF as

$$G(\mathbf{x}) = S \exp\left(-\frac{x_1^2}{2\sigma_1^2} - \frac{x_2^2}{2\sigma_2^2}\right) \cos(2\pi|\mathbf{f}^{\text{RF}}|x_1 + \phi^{\text{RF}})$$

S determines the overall strength, σ_1 and σ_2 determine the size, and ϕ^{RF} the spatial phase of the Gabor RF. Positive values of the Gabor, $G^+(\mathbf{x}) = \max[G(\mathbf{x}), 0]$, give the connection strength from ON cells, whereas the magnitude of the negative values, $G^-(\mathbf{x}) = |\min[G(\mathbf{x}), 0]|$, gives the connection strength from OFF cells. Note that $G(\mathbf{x}) = G^+(\mathbf{x}) - G^-(\mathbf{x})$, while $|G(\mathbf{x})| =$

$G^+(\mathbf{x}) + G^-(\mathbf{x})$. Using a linear summation model, the total input to the cortical cell is given by

$$\begin{aligned}
 I_{\text{LGN}} &= \int d\mathbf{x} G^+(\mathbf{x}) L^{\text{ON}}(\mathbf{x}) + G^-(\mathbf{x}) L^{\text{OFF}}(\mathbf{x}) \\
 &= \int d\mathbf{x} G^+(\mathbf{x}) [L^{\text{avg}}(\mathbf{x}) + L^{\text{diff}}(\mathbf{x})] + G^-(\mathbf{x}) [L^{\text{avg}}(\mathbf{x}) - L^{\text{diff}}(\mathbf{x})] \\
 &= \int d\mathbf{x} [G^+(\mathbf{x}) - G^-(\mathbf{x})] L^{\text{diff}}(\mathbf{x}) + [G^+(\mathbf{x}) + G^-(\mathbf{x})] L^{\text{avg}}(\mathbf{x}) \\
 &= \int d\mathbf{x} G(\mathbf{x}) L^{\text{diff}}(\mathbf{x}) + |G(\mathbf{x})| L^{\text{avg}}(\mathbf{x}) \tag{2}
 \end{aligned}$$

Thus the total input to a simple cell can be written as the sum of two components: the result of a Gabor filter applied to one-half the difference of ON and OFF cell responses, plus the result of a filter obtained from the absolute value of the Gabor applied to the average of ON and OFF cell responses. We will call these the ON/OFF-specific and ON/OFF-averaged components of the input, and will call $|G(\mathbf{x})|$ the absolute Gabor filter.

In the common linear model of LGN input, the firing rate modulation of OFF cells is assumed equal and opposite to ON cell modulations at a given point \mathbf{x} . Therefore $L^{\text{avg}}(\mathbf{x})$ is a constant equal to the average background firing rate of LGN cells, and the ON/OFF-averaged term contributes only a stimulus-independent background input to the cortex. As a result, the linear model only considers the ON/OFF-specific component of the LGN input. However, since LGN firing rates cannot be modulated below 0 Hz, at higher contrasts the balance between ON and OFF cell modulations cannot be maintained, and the ON/OFF-averaged term grows with increasing contrast. Hence it becomes important to retain both terms in modeling LGN input.

Further insight into this decomposition can be gained by considering, for any given cortical cell, the cell's *antiphase partner*: an imaginary cell that has identical Gabor receptive field except for an overall sign reversal, so that ON subregions (connections from ON cells) are replaced with OFF subregions (connections from OFF cells) and vice versa. Then the ON/OFF-specific term represents the component of LGN input that is equal and opposite to a cell and to its antiphase partner, while the ON/OFF-averaged term represents the input component that is identical to a cell and to its antiphase partner. It is in this sense that we call these the *ON/OFF-specific* and *ON/OFF-averaged* input components, respectively. The decomposition into these two components is key to the results presented below.

Input from grating stimuli

In this paper, we focus on responses to periodic gratings, i.e., stimuli that are spatially periodic in one dimension and uniform in the other dimension. The periodicity of the gratings is described by a two-dimensional spatial frequency vector \mathbf{f}^{stim} , and we assume that LGN cells have circularly symmetric receptive fields. Therefore the response of an LGN ON-center cell is determined by its position relative to the grating: $L^{\text{ON}}(\mathbf{x}) = l^{\text{ON}}(\mathbf{f}^{\text{stim}} \cdot \mathbf{x})$, where $l^{\text{ON}}(\phi)$ is some function of a scalar variable ϕ determining a cell's location relative to the periodic modulation of the overall LGN activity pattern. Sim-

ilarly, $L^{\text{OFF}}(\mathbf{x}) = l^{\text{OFF}}(\mathbf{f}^{\text{stim}} \cdot \mathbf{x})$. Throughout we will assume $|\mathbf{f}^{\text{stim}}| = |\mathbf{f}^{\text{RF}}|$. LGN spatial frequency tuning can be included by writing $L^{\text{ON}}(\mathbf{x}) = F^{\text{ON}}(|\mathbf{f}^{\text{stim}}|) l^{\text{ON}}(\mathbf{f}^{\text{stim}} \cdot \mathbf{x})$, where $F^{\text{ON}}(|\mathbf{f}^{\text{stim}}|)$ is the spatial frequency tuning of ON cells scaled so that $F^{\text{ON}}(|\mathbf{f}^{\text{RF}}|) = 1$. Similar definitions apply for OFF cells.

Given that LGN activity is periodic with spatial frequency \mathbf{f}^{stim} , the $L^{\text{avg}}(\mathbf{x})$ and $L^{\text{diff}}(\mathbf{x})$ components of LGN activity can each be written as a cosine series

$$\begin{aligned}
 L^{\text{diff}}(\mathbf{x}) &= \sum_{n=0}^{\infty} a_n^{\text{diff}} \cos [n(2\pi \mathbf{f}^{\text{stim}} \cdot \mathbf{x}) + \hat{\phi}_n^{\text{diff}}] \\
 L^{\text{avg}}(\mathbf{x}) &= \sum_{n=0}^{\infty} a_n^{\text{avg}} \cos [n(2\pi \mathbf{f}^{\text{stim}} \cdot \mathbf{x}) + \hat{\phi}_n^{\text{avg}}]
 \end{aligned}$$

Here, $0 \leq \hat{\phi}_n^{\text{diff}} < 2\pi$ and $0 \leq \hat{\phi}_n^{\text{avg}} < 2\pi$ represent the phase of each component.

Using these expansions, we can evaluate the integral in Eq. 2 and rewrite the total LGN input to a simple cell as the sum of a pair of cosine series

$$I_{\text{LGN}} = \sum_{n=0}^{\infty} \mathcal{G}(n\mathbf{f}^{\text{stim}}) a_n^{\text{diff}} \cos(\phi_n^{\text{diff}}) + \sum_{n=0}^{\infty} |\mathcal{G}(n\mathbf{f}^{\text{stim}})| a_n^{\text{avg}} \cos(\phi_n^{\text{avg}}) \tag{3}$$

$\mathcal{G}(n\mathbf{f}^{\text{stim}})$ and $|\mathcal{G}(n\mathbf{f}^{\text{stim}})|$ are the amplitudes of the Gabor and absolute Gabor filters, respectively, evaluated at the spatial frequency vector $n\mathbf{f}^{\text{stim}}$ (i.e., the amplitudes of the Fourier transforms of G and $|G|$ at this frequency). The phases are $\phi_n^{\text{diff}} = \hat{\phi}_n^{\text{diff}} + \phi_n^G$ and $\phi_n^{\text{avg}} = \hat{\phi}_n^{\text{avg}} + \phi_n^{|G|}$, where ϕ_n^G and $\phi_n^{|G|}$ are the phases contributed by the Gabor and absolute Gabor filters.

We reiterate that our model is a spatial model. The instantaneous spatial distribution of activity across a two-dimensional sheet of LGN cells (described by a^{diff} and a^{avg}) is multiplied by the appropriate Gabor filters to determine the total LGN input to a cortical cell at a given time, and the cortical response is assumed to depend instantaneously on this input. For temporal patterns of input, such as a drifting or counterphased grating, we simply assume that the cortical responses can be computed as instantaneous responses to a sequence of patterns of LGN activity that change in time. For flashed stimuli, the model will apply to the degree that cortical responses simply track the changing patterns of LGN activity triggered by the flash.

Reduction to two terms

In this subsection, we argue that each of the two sums in Eq. 3 should be dominated by the contribution of a single term. In particular, the ON/OFF-averaged sum is dominated by the zero frequency (DC) term, and the ON/OFF-specific sum is dominated by the first harmonic (F1) term. Having shown that this is the case, we will have demonstrated that

$$I_{\text{LGN}} \cong \text{DC} + \text{F1} \cos(\phi_{\text{stim}}) \tag{4}$$

where we have defined the phase of the stimulus to equal the phase of the spatial modulation of LGN activity ($\phi_{\text{stim}} \equiv \phi_1^{\text{diff}}$). The dominance of the DC and F1 terms depends on a *quantitative* examination of Eq. 3. Therefore we will evaluate the relative magnitudes of the first six terms in each cosine series, using a simple model of LGN responses to sinusoidal gratings.

“DC” will be used to refer to the amplitude of the zero frequency component ($n = 0$) of a cosine expansion, and “ F_n ” to refer to the amplitude of the n th harmonic (e.g., F_1 for $n = 1$).

We consider a simple rectified-linear model of LGN responses. ON and OFF cells are assumed to have background firing rates of 10 and 15 Hz, respectively, and response modulations are assumed to result from linear filter properties of the LGN cells. Therefore a drifting sinusoidal grating stimulus leads individual LGN cells to sinusoidally modulate their firing rates with time, rectified at 0 Hz (Fig. 1, A and B). This means that at each instant the spatial pattern of response across the sheet of LGN cells is a rectified sinusoidal modulation. The amplitude of the modulation of activity across LGN depends on the contrast of the grating (Fig. 1C) and was calculated using measured contrast response functions from cat LGN X cells in response to drifting sinusoidal gratings. The phase of the modulation is assumed opposite (180° apart) for an ON cell and an OFF cell at the same position. This ignores the actual spread of response phases for both ON and OFF cells (Saul and Humphrey 1990; Wolfe and Palmer 1998). At low contrasts, the stimulus-induced modulations of firing rates do not exceed the background firing rates, and so the mean input does not grow with contrast. However, once the stimulus-induced modulation is as large as the background firing rates—which occurs at about 5% contrast—then the LGN firing rates rectify at 0 Hz for each trough of the modulation (Fig. 1), and so increases in contrast above 5% lead to an increase in the mean LGN input.

Using the measured contrast response functions, we compute the magnitudes of a_n^{diff} and a_n^{avg} for a sinusoidal stimulus grating at 20% contrast (white bars in Fig. 2, A and B, respectively). The difference coefficients, a_n^{diff} , are small for n even. This is because the difference between ON and OFF cell re-

sponses during the first half of a response cycle is nearly equal and opposite to the response difference during the second half of the cycle. The dominance of the difference by the F_1 coefficient, a_1^{diff} , results from the fact that LGN response modulations take the shape of a rounded “hump” of increased firing rate occurring during each cycle of the stimulus grating. The DC contribution, a_0^{diff} , is largely due to the difference between the background firing rates of ON and OFF cells. Examining the average coefficients, a_n^{avg} , we see that the DC contribution dominates, with a smaller contribution from the first few harmonics. The dominance of the average by the DC component follows from the fact that each hump of ON or OFF cell activity fills out at least one-half of the cycle, and hence the average activity undergoes only small modulation.

We now turn our attention to the Gabor filters. Since a Gabor function is obtained by multiplying a sinusoid and a Gaussian, the Fourier transform of G consists of a Gaussian convolved with a pair of delta functions located at the positive and negative frequencies of the sinusoid (Fig. 2C). The specific parameter values used have been extracted from two sets of experimental data. We started with Gabor parameters taken as the mean values from measured simple cell RFs [Jones and Palmer (1987b); full parameters are given in METHODS section of Troyer et al. (1998)]. The length of each subregion was then reduced so that the orientation tuning width of the F_1 of the total LGN input (38.0° half-width at half-height) matched the mean tuning width of experimentally measured intracellular voltage (Carandini and Ferster 2000). This was accomplished by multiplying the standard deviation of the Gaussian envelope in the direction parallel to the subregion by a factor of 0.58. One important feature to note is that the width of the Gaussian in Fourier space is similar to the preferred spatial frequency of the Gabor RF. This condition will hold when the simple cell RF has roughly two subregions; more subregions will narrow this width. The absolute value of the Gabor, $|G|$, is obtained by multiplying a Gaussian times the absolute value of a sinusoid. Thus the Fourier transform $|\mathcal{G}|$ consists of a Gaussian convolved with the Fourier series for the absolute value of a sinusoid, which has only even harmonics (Fig. 2C). We focus on the response at the optimal orientation, and fix the stimulus spatial frequency to match the optimal spatial frequency of the Gabor filter, i.e., $f^{\text{stim}} = f^{\text{RF}}$. In this case, the multiples of the stimulus spatial frequency vector, nf^{stim} , fall on the peaks of the Gaussian-shaped humps in the Gabor and absolute Gabor filters (Fig. 2, A and B, marked x). The result is that the $\mathcal{G}(nf^{\text{stim}})$ coefficients are dominated by the F_1 ($n = 1$) component (Fig. 2A, gray bars), while the $|\mathcal{G}|(nf^{\text{stim}})$ coefficients are dominated by the DC ($n = 0$) component (Fig. 2B, gray bars).

Having calculated the values a_n^{diff} , a_n^{avg} , $\mathcal{G}(nf^{\text{stim}})$ and $|\mathcal{G}|(nf^{\text{stim}})$, we need only multiply the corresponding components to calculate the ON/OFF-specific and ON/OFF-averaged components of the total LGN input using Eq. 3. The results, shown by the black bars in Fig. 2, A and B, demonstrate that only two terms contribute significantly to the total LGN input. Since both the Gabor filter \mathcal{G} and the Fourier series for L^{diff} are dominated by the F_1 component, 99.9% of the total power in the diff terms is concentrated in the first harmonic. Similarly, the avg terms are dominated by the DC, with 98.6% of the power concentrated in the zero frequency (mean) component of the input. Thus the approximation given by Eq. 4 is valid for

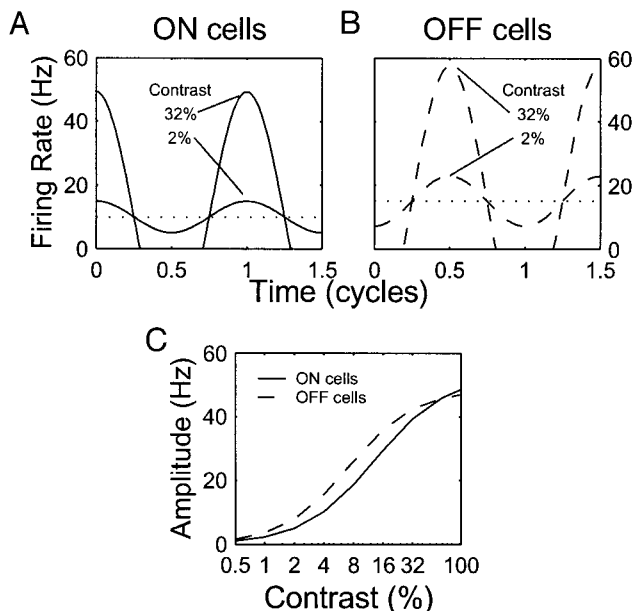


FIG. 1. Linear rectified model of lateral geniculus (LGN) response to drifting sinusoidal gratings. A and B: response of ON and OFF cells to drifting sinusoidal gratings of 2 and 32% contrast. C: modulation amplitude as a function of contrast for ON and OFF cells (computed from F_1 of spiking response from Cheng et al. 1995, assuming background firing rates of 10 and 15 Hz, respectively, and a linear rectified model of LGN response; see METHODS in Troyer et al. 1998).

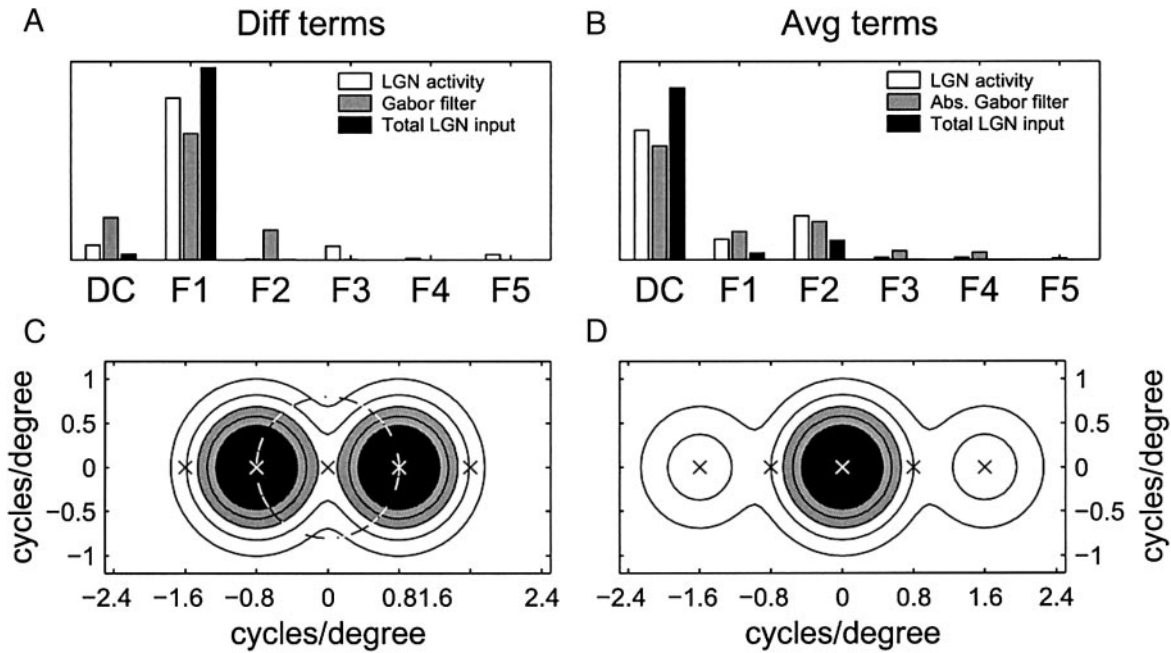


FIG. 2. Spatial frequency components of the contributions to the LGN input I_{LGN} , for LGN response model shown in Fig. 1 at 20% contrast. *Top*: amplitude of coefficients of *diff* terms (A) and *avg* terms (B) in Eq. 3, for a sinusoidal grating stimulus. White bars: magnitudes of a_n^{diff} or a_n^{avg} . Gray bars: magnitudes of $\mathcal{G}(n\mathbf{f}^{\text{stim}})$ or $|\mathcal{G}(n\mathbf{f}^{\text{stim}})|$, when the stimulus is at the Gabor's preferred orientation. Black bars: magnitudes of the corresponding component of I_{LGN} , i.e., of the product $a_n^{\text{diff}}\mathcal{G}(n\mathbf{f}^{\text{stim}})$ or $a_n^{\text{avg}}|\mathcal{G}(n\mathbf{f}^{\text{stim}})|$. Gray, white, and black bars in A and B are separately scaled to yield the same total length. *Bottom*: contour plot of Gabor filter (C) and absolute Gabor filter (D). Multiples of preferred spatial frequency (0.8 cycles/degree) at the preferred orientation are marked x. Circle in C shows the location of the stimulus 1st harmonic as the stimulus ranges over all orientations.

the rectified-linear model of LGN response used here, with $\text{DC} = |\mathcal{G}(0)a_0^{\text{avg}}|$ and $\text{F1}(C, \theta) = \mathcal{G}(\mathbf{f}^{\text{stim}})a_1^{\text{diff}}$.

Thus we have shown that the total LGN input to a cortical simple cell in response to a periodic grating (Eq. 3) is expected to be well-approximated by a sinusoidal modulation about some mean level (Eq. 4). This was derived assuming a linear-rectified LGN response model and a sinusoidal grating, but is likely to hold for more general LGN response models and for more general types of gratings. So long as the F1 of L^{diff} is at least as large as the other Fourier coefficients, the dominance of the F1 in the Gabor filter will lead the ON/OFF-specific terms to be dominated by the F1. Similarly, the ON/OFF-averaged components will be dominated by the DC so long as the DC of L^{avg} is at least as large as the other Fourier coefficients.

Orientation tuning

We now examine the orientation and contrast dependence of the DC and F1 terms of the total LGN input. We express the orientation θ in degrees from the preferred orientation, i.e., 0 degrees is the optimal stimulus. Since the responses of individual LGN cells are untuned for orientation, changing the orientation of the stimulus will rotate this activity pattern, but will leave the shape of the activity modulation unchanged. Therefore the coefficients a_n^{diff} and a_n^{avg} that characterize the activity modulation in response to a given stimulus do not depend on stimulus orientation. Because we are assuming that the spatial frequency $|\mathbf{f}^{\text{stim}}|$ is fixed, the only remaining stimulus parameter is the contrast, so we can write $a_n^{\text{avg}} = a_n^{\text{avg}}(C)$, $a_n^{\text{diff}} = a_n^{\text{diff}}(C)$. Therefore the DC term in Eq. 4 can be written as

$$\text{DC}(C, \theta) = |\mathcal{G}(0)a_0^{\text{avg}}(C)| = \text{DC}(C) \quad (5)$$

That is, the DC term is untuned for orientation. This is a mathematical restatement of the fact that the mean LGN input to a cortical simple cell is equal to the sum of the mean responses of its LGN input cells, weighted by their connection strength. Because the mean response of each LGN cell is orientation independent, so is the weighted sum of these mean responses. Note that the DC term *does* depend on contrast, since rectification makes average LGN activity increase with increasing contrast for contrasts above 5% (Fig. 1).

We now turn our attention to the F1 term. First, we write the spatial frequency vector of the stimulus in polar coordinates, $\mathbf{f}^{\text{stim}} = \{|\mathbf{f}^{\text{stim}}|, \theta\}$ and let $\mathcal{G}_0 = \mathcal{G}(\{|\mathbf{f}^{\text{stim}}|, 0\})$. Then we factor the amplitude of the modulation as follows

$$\begin{aligned} \text{F1}(C, \theta) &= \mathcal{G}(\{|\mathbf{f}^{\text{stim}}|, \theta\})a_1^{\text{diff}}(C) \\ &= \mathcal{G}_0a_1^{\text{diff}}(C)\mathcal{G}(\{|\mathbf{f}^{\text{stim}}|, \theta\})/\mathcal{G}_0 \\ &= \text{F1}_{\text{max}}(C)h(\theta) \end{aligned} \quad (6)$$

$\text{F1}_{\text{max}}(C) = \mathcal{G}_0a_1^{\text{diff}}(C)$ captures the contrast response at the preferred orientation, and $h(\theta) = \mathcal{G}(\{|\mathbf{f}^{\text{stim}}|, \theta\})/\mathcal{G}_0$ captures the orientation tuning of the Gabor RF, normalized so that at the preferred orientation, $h(0) = 1$. Therefore the total LGN input can be written in its final form

$$I_{\text{LGN}}(C, \theta, t) \cong \text{DC}(C) + \text{F1}_{\text{max}}(C)h(\theta) \cos(\phi_{\text{stim}}) \quad (7)$$

$h(\theta)$ is determined by the evaluation of the filter G along the circle of radius $|\mathbf{f}^{\text{stim}}|$ (Fig. 2C). If the Gabor RF has two or more subregions and the spatial frequency $|\mathbf{f}^{\text{stim}}| = |\mathbf{f}^{\text{RF}}|$, $h(\theta)$ is dominated by the contribution from the Gaussian centered at \mathbf{f}^{RF} . In this case

$$h(\theta) \approx \exp\{-[|\mathbf{f}^{\text{RF}}| - |\mathbf{f}^{\text{stim}}| \cos(\theta)]^2/(2\sigma_x^2) - [|\mathbf{f}^{\text{stim}}| \sin(\theta)]^2/(2\sigma_y^2)\} \quad (8)$$

where $\tilde{\sigma}_x = 1/\sigma_x$ and $\tilde{\sigma}_y = 1/\sigma_y$ determine the dimensions of the Gaussian envelope of the Gabor filter in Fourier space. For $|\mathbf{f}^{\text{stim}}| \neq |\mathbf{f}^{\text{RF}}|$, $h(\theta)$ takes on a more complex form. Qualitatively, tuning narrows for $|\mathbf{f}^{\text{stim}}| > |\mathbf{f}^{\text{RF}}|$ and broadens for $|\mathbf{f}^{\text{stim}}| < |\mathbf{f}^{\text{RF}}|$.

This concludes our analysis of the LGN input to a simple cell. We now turn to the analysis of the conditions yielding contrast-invariant orientation tuning.

CONTRAST-INVARIANT ORIENTATION TUNING I: HIGHER-CONTRAST REGIME

Intracortical inhibition

A key to our model of contrast-invariant orientation tuning at higher contrasts is the inclusion of strong, contrast-dependent feed-forward inhibition. We will take the inhibition a cell receives to be spatially opponent to, or antiphase relative to, the excitation a cell receives; this is also known as a push-pull arrangement of excitation and inhibition. By spatial opponency of inhibition and excitation, we mean that in an ON subregion of the simple cell RF, where increases in luminance evoke excitation [i.e., where $G^+(\mathbf{x}) > 0$], decreases in luminance evoke inhibition; the opposite occurs in OFF subregions [where $G^-(\mathbf{x}) > 0$]. Since the LGN projection to cortex is purely excitatory (Ferster and Lindström 1983), this inhibition must come from inhibitory interneurons in the cortex. A simple hypothesis that is consistent with a broad range of experimental data is that a given simple cell receives input from a set of inhibitory simple cells that collectively 1) have RFs roughly overlapping that of the simple cell, 2) are tuned to a similar orientation as the simple cell, and 3) have OFF subregions roughly overlapping the simple cell's ON subregions, and vice versa (Troyer et al. 1998); that is, collectively a cell's inhibitory input has a receptive field like that of a cell's "antiphase partner." This circuitry leads to inhibition that, like the inhibition observed physiologically, is spatially opponent to the excitation a cell receives (Anderson et al. 2000a; Ferster 1988; Hirsch et al. 1998), and has the same preferred orientation and tuning width as a cell's excitatory inputs from the LGN (Anderson et al. 2000a; Ferster 1986).

The role of antiphase inhibition in cortical orientation tuning can be understood quite generally by returning to our decomposition of the LGN input into an ON/OFF-specific term and an ON/OFF-averaged term. The ON/OFF-specific component typically is tuned for stimulus parameters such as orientation while the ON/OFF-averaged component typically is untuned or poorly tuned. The ON/OFF-specific term represents input that is equal and opposite to a cell and to its antiphase partner. Thus, for this component, the antiphase inhibition goes down when LGN excitation goes up, and vice versa. The net result is that strong antiphase inhibition serves to amplify the well-tuned ON/OFF-specific component of the LGN input. The ON/OFF-averaged term represents input that is identical to a cell and to its antiphase partner. If the antiphase inhibition is stronger than the direct LGN excitation, the ON/OFF-averaged term elicits a net inhibitory input that is poorly tuned for orientation but depends on contrast. Thus antiphase inhibition serves to eliminate the untuned component of the LGN input and replace it with a net inhibition that sharpens the spiking responses driven by

the ON/OFF-specific tuned component of the input. This argument generalizes to any type of stimulus, transient or sustained. We now work out the details of this for the case of a drifting sinusoidal grating stimulus.

In our reduced model, we represent the set of inhibitory cells providing inhibition to a cell by a single inhibitory simple cell. This cell receives input from the LGN specified by a Gabor function identical to that which specifies the input to the excitatory cell except that the sinusoidal modulation of the RF is 180° out of phase. The total LGN input to the inhibitory cell is then

$$\begin{aligned} I_{\text{inh}}(C, \theta, \phi_{\text{stim}}) &\equiv \text{DC}(C) + F1_{\text{max}}(C)h(\theta) \cos(\phi_{\text{stim}} + 180^\circ) \\ &= \text{DC}(C) - F1_{\text{max}}(C)h(\theta) \cos(\phi_{\text{stim}}) \end{aligned}$$

For now, we will assume that the output spike rates for cortical neurons result from a rectified-linear function of the neuron's input. The effects of smoothing this function will be considered in the section on the *Low-contrast regime*. Given this assumption, the inhibitory cell's firing rate is

$$r_{\text{inh}}(C, \theta, \phi_{\text{stim}}) = g_{\text{inh}}|\text{DC}(C) - F1_{\text{max}}(C)h(\theta) \cos(\phi_{\text{stim}}) + b_{\text{inh}} - \psi_{\text{inh}}|^+ \quad (9)$$

where $| \cdot |^+$ denotes rectification, g_{inh} is the gain of the input/output function for the inhibitory cell, ψ_{inh} is spike threshold, and b_{inh} is the amount of nonspecific input received at background. For simplicity, we assume that input to the inhibitory cell never dips below threshold [i.e., $\text{DC}(100) - F1_{\text{max}}(100) + b_{\text{inh}} - \psi_{\text{inh}} \geq 0$], allowing us to ignore inhibitory cell rectification. This assumption is not unreasonable given the experimental evidence suggesting that some inhibitory interneurons have high background firing rates (Brumberg et al. 1996; Swadlow 1998). Moreover, the more realistic version of the model presented in Troyer et al. (1998) included inhibitory cell rectification, and this had no significant impact on our results.

It is important to note that the model inhibitory cell responds to *all* orientations, although it also shows orientation tuning. For nonpreferred orientations, for which $h(\theta) \approx 0$, the cell still receives positive input due to the term $\text{DC}(C)$ in Eq. 9, which drives inhibitory response. This inhibition is critical for overcoming the strong, contrast-dependent LGN excitation that would otherwise drive excitatory simple cells at the null orientation. The DC term contributes an untuned platform to the inhibitory cell orientation tuning curve, identical for all orientations, on which the tuned response component due to the term containing $h(\theta)$ is superimposed. That is, the inhibitory cell tuning follows the tuning of the total LGN input to a simple cell, which includes both an untuned and a tuned component. One of the key predictions of our model (Troyer et al. 1998) was that there should be at least a subset of layer 4 interneurons that show contrast-dependent responses to all orientations (see DISCUSSION), which is embodied here in the response of our single model inhibitory neuron.

To facilitate analysis, we assume that excitation and inhibition combine linearly, at least in their effect on spiking output. Because this assumption ignores reversal potential nonlinearities, the total input in our model should not be equated with the membrane voltage, particularly for voltages near the inhibitory reversal potential (see DISCUSSION). Letting \tilde{w} denote the

strength of the inhibitory connection, the total input to the excitatory simple cell is

$$\begin{aligned}
 I(C, \theta, \phi_{\text{stim}}) &= I_{\text{LGN}}(C, \theta, \phi_{\text{stim}}) - \bar{w}r_{\text{inh}}(C, \theta, \phi_{\text{stim}}) \\
 &= \text{DC}(C) + \text{F1}_{\text{max}}(C)h(\theta) \cos(\phi_{\text{stim}}) \\
 &\quad - \bar{w}g_{\text{inh}}[\text{DC}(C) - \text{F1}_{\text{max}}(C)h(\theta) \cos(\phi_{\text{stim}}) + b_{\text{inh}} - \psi_{\text{inh}}] \\
 &= (1 - w)\text{DC}(C) + (1 + w)\text{F1}_{\text{max}}(C)h(\theta) \cos(\phi_{\text{stim}}) \\
 &\quad - w(b_{\text{inh}} - \psi_{\text{inh}}) \tag{10}
 \end{aligned}$$

where we let $w = \bar{w}g_{\text{inh}}$ denote the total gain of the feed-forward inhibition, i.e., w depends on the transformation of LGN input to inhibitory spike rate as well as on inhibitory synaptic strength. Note that *Eq. 10* assumes that disynaptic inhibition arrives simultaneously with direct LGN excitation. In reality there is a small time lag: in response to flashed stimuli, feed-forward inhibition takes about 2 ms longer to arrive than feed-forward excitation (Hirsch et al. 1998). This lag is likely to be negligible even for transient stimuli and is certainly negligible for drifting gratings at frequencies that drive cells in cat V1 (<10 Hz). In addition, for drifting gratings, even a larger lag would serve only to reduce the amplification of the modulation term due to withdrawal of inhibition, since the DC term is time independent by definition.

Inhibition has opposite effects on the DC and F1 terms of the total input: it acts to suppress the mean input [DC \rightarrow (1 - w)DC], while it enhances the modulation [F1 \rightarrow (1 + w)F1]. The increase in the modulation is due to the fact that, at any given contrast, increases in LGN excitation are accompanied by a withdrawal of cortical inhibition, while decreases of excitation are accompanied by an increase of inhibition. A key requirement of our model of contrast-invariant tuning is that the inhibition be dominant ($w > 1$), i.e., the inhibitory input is stronger than the direct input from the LGN. This implies that the contrast-dependent increase in the mean input from the LGN is not only suppressed, it is actually reversed (1 - $w < 0$), so that the mean feed-forward input to the cortical simple cell *decreases* with increasing contrast.

Contrast invariance

Given the assumption that output spike rate results from a rectified linear function of the input, the excitatory spike rate is

$$r(C, \theta, \phi_{\text{stim}}) = g[(1 - w)\text{DC}(C) + (1 + w)\text{F1}_{\text{max}}(C)h(\theta) \cos(\phi_{\text{stim}}) - \psi^{\text{eff}}]^+ \tag{11}$$

where $\psi^{\text{eff}} = \psi_{\text{exc}} - b_{\text{exc}} + w(b_{\text{inh}} - \psi_{\text{inh}})$ is an effective threshold that incorporates tonic inhibitory activity, nonspecific input to the excitatory cell b_{exc} and the excitatory-cell spike threshold ψ_{exc} . Note that, after specifying the Gabor RF, the cortical component of our model has only two free parameters, w and ψ^{eff} ; the gain factor g is simply a scale factor that determines the magnitude of response without affecting tuning.

For the orientation tuning of the response to be contrast invariant, we must be able to write $r(C, \theta, \phi_{\text{stim}})$ as the product of a contrast response function $p(C)$ and an orientation tuning function $q(\theta, \phi_{\text{stim}})$. Since the F1 term is the only term that depends on the orientation and phase of the stimulus, we look for an expression of the form

$$q(\theta, \phi_{\text{stim}}) = g[(1 + w)h(\theta) \cos(\phi_{\text{stim}}) + z]^+$$

where z is some constant. Then we would have

$$r(C, \theta, \phi_{\text{stim}}) \equiv p(C)q(\theta, t) = g[p(C)(1 + w)h(\theta) \cos(\phi_{\text{stim}}) + p(C)z]^+ \tag{12}$$

Identifying the terms of this equation with the terms of *Eq. 11* yields

$$\begin{aligned}
 p(C) &= \text{F1}_{\text{max}}(C) \\
 p(C)z &= (1 - w)\text{DC}(C) - \psi^{\text{eff}} \tag{13}
 \end{aligned}$$

Together these imply the following simple condition that, if satisfied for some constant $k = z/(1 - w)$, guarantees that the response is contrast invariant

$$k\text{F1}_{\text{max}}(C) = \text{DC}(C) + \psi^{\text{eff}}/(w - 1) \tag{14}$$

Equation 14 implies growth of the DC term with contrast, and hence can only hold for contrasts above 5%, for which LGN firing rates rectify at 0 so that their mean rates increase with contrast. This equation also demonstrates that the inhibitory strength w determines the width of the tuning curve. Focusing on the optimal phase of the response [$\cos(\phi_{\text{stim}}) = 1$], suprathreshold responses require $h(\theta) > k(w - 1)/(w + 1)$. For larger values of inhibitory strength w , $h(\theta)$ has to be closer to its maximum value before threshold is crossed, i.e., tuning width is narrower.

Equation 14 implies a strong version of contrast-invariant tuning. Not only is the tuning of average spike rate contrast invariant, but the spike rate at any given phase of the response at a given orientation multiplicatively scales with changes in contrast.

Parameter dependence

Equation 14 is equivalent to the statement that the DC and F1 terms have the same *shape* as functions of contrast, up to a scale factor determined by k and an offset determined by $\psi^{\text{eff}}/(w - 1)$. Using *Eqs. 5* and *6*, *Eq. 14* can be rewritten

$$|g|(0)a_0^{\text{avg}}(C) = k|g|(|f^{\text{stim}}|, 0)a_1^{\text{diff}}(C) - \psi^{\text{eff}}/(w - 1) \tag{15}$$

Equation 15, similarly to *Eq. 14*, implies that $a_0^{\text{avg}}(C)$ and $a_1^{\text{diff}}(C)$ must have the same shape as functions of contrast, up to a scale factor and offset. Using our linear-rectified model of LGN response, we can plot $a_0^{\text{avg}}(C)$ and $a_1^{\text{diff}}(C)$ versus contrast C (*Fig. 3A*). After a suitable scaling and offset, the two overlap

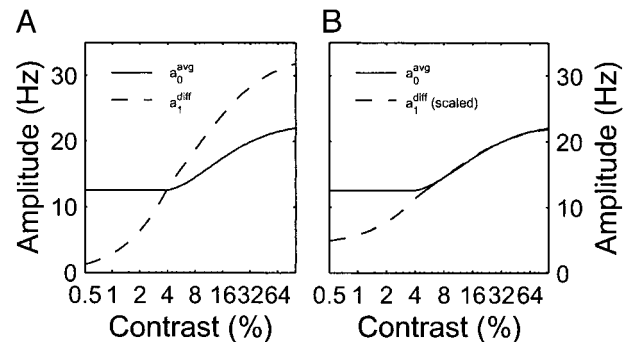


FIG. 3. The condition for contrast invariance is satisfied above 5% Contrast. A: a_0^{avg} and a_1^{diff} as functions of contrast for the linear rectified LGN responses to drifting sinusoidal gratings shown in *Fig. 1*. B: $a_0^{\text{avg}}(C)$ and a rescaled and offset version of $a_1^{\text{diff}}(C)$ [$0.56 + 4.16a_1^{\text{diff}}(C)$ - determined by a linear regression calculated at 50 contrasts equally spaced on a log scale between 5 and 100% contrast].

almost perfectly at contrasts above 5% (Fig. 3B), and thus the condition for contrast invariance is met at these contrasts. At contrasts below 5%, LGN responses do not rectify and the mean response, $a_0^{\text{avg}}(C)$, does not change with contrast. Since $a_0^{\text{avg}}(C)$ and $a_1^{\text{diff}}(C)$ diverge, contrast invariance in our model fails at low contrast. This failure will be remedied below by consideration of the effects of noise on the response.

Figure 3 shows, for our linear-rectified model of LGN response, that $a_0^{\text{avg}}(C)$ and $a_1^{\text{diff}}(C)$ have the same shape as a function of contrast. As a result, Eq. 15 can be satisfied and contrast invariance achieved, provided the two parameters of our model, the inhibitory strength w and the effective threshold ψ^{eff} , are chosen to satisfy Eq. 15 for some constant k . To determine the robustness of our model, we simply varied these two parameters and measured the resulting contrast dependence of orientation tuning. We consider three levels of inhibition (left to right columns of Fig. 4) and three levels of effective threshold (thick, thin, and dashed lines in Fig. 4, where the thick line represents the optimal threshold for achieving contrast-invariant tuning for that level of inhibition). The orientation tuning width, as measured by half width at half height of the orientation tuning curve, is contrast invariant down to about 5% contrast for the optimal threshold, as expected (Fig. 4B). With nonoptimal thresholds, modest deviations from contrast invariance arise in the range of 5–10% contrast.

Contrast invariance: an intuitive explanation

From Fig. 4A we can obtain an intuitive picture of how our model achieves contrast-invariant orientation tuning in the higher-contrast regime. Since the magnitude of the input modulation increases with increasing contrast, the tuned component of the total input also increases. However, with dominant inhibition, the mean input *decreases* with increasing contrast, so that the growing tuned component rides on a “sinking” untuned platform. Thus there will be some orientation where the input tuning curve for a higher contrast stimulus will cross the corresponding curve for a low contrast stimulus (Fig. 4A). Placing spike threshold at the level where the contrast-dependent tuning curves cross then yields contrast-invariant responses (Fig. 4, A and B, thick lines). Note that as the level of

inhibition increases, the crossing point of the input tuning curves occurs closer to the peak, resulting in narrower tuning.

The fact that this crossing point occurs at the same orientation across a range of contrasts is exactly equivalent to the condition that $a_0^{\text{avg}}(C)$ and $a_1^{\text{diff}}(C)$ have the same shape as functions of contrast. Figure 3 shows that $a_0^{\text{avg}}(C)$ and $a_1^{\text{diff}}(C)$ do indeed have the same shape as functions of contrast (at contrasts above 5%), at least for a particular model of LGN response. To determine whether contrast invariance is likely to hold for a range of models, it is important to understand the underlying reasons why $a_0^{\text{avg}}(C)$ and $a_1^{\text{diff}}(C)$ have the same shape as functions of contrast. The answer becomes clear if we consider a_0^{avg} and a_1^{diff} not as functions of contrast, but as functions of the peak of the LGN response. At high contrast, our model LGN responses are reasonably well-approximated by a half-wave rectified sinusoid. Therefore a_0^{avg} and a_1^{diff} should both be nearly linear functions of the peak LGN response, which implies that they both have the same shape as a function of contrast. The dependence of a_0^{avg} and a_1^{diff} on peak LGN amplitude is plotted in Fig. 5, and indeed both show nearly linear dependence at contrasts above 5%. While this was computed using our linear-rectified LGN model, the result is more general: as long as the LGN response can be approximated as a rounded “hump” of activity that does not drastically alter its shape with changes in contrast, the DC and F1 will grow nearly linearly with the size of the hump. Since sensitivity to the exact placement of threshold is weak, contrast invariance is expected to hold for a wide range of models in which LGN responses rectify.

Given this intuitive picture, it is clear that the crucial role for inhibition in our model is to counteract the untuned component of LGN excitation and convert it into an untuned suppression that acts like a contrast-dependent threshold. In our push-pull model, this inhibition comes from the cell’s antiphase partner and is directly driven by the untuned component of the LGN input. Other sources of this inhibition are possible, such as complex inhibitory cells that are untuned for orientation (Hirsch et al. 2000), or inhibition coming from simple cells having a range of spatial phases (McLaughlin et al. 2000; Wiesel et al. 2001) (see DISCUSSION). The key properties of the inhibition for our model are that it should be able to cancel the large, contrast-dependent LGN input expected at the null

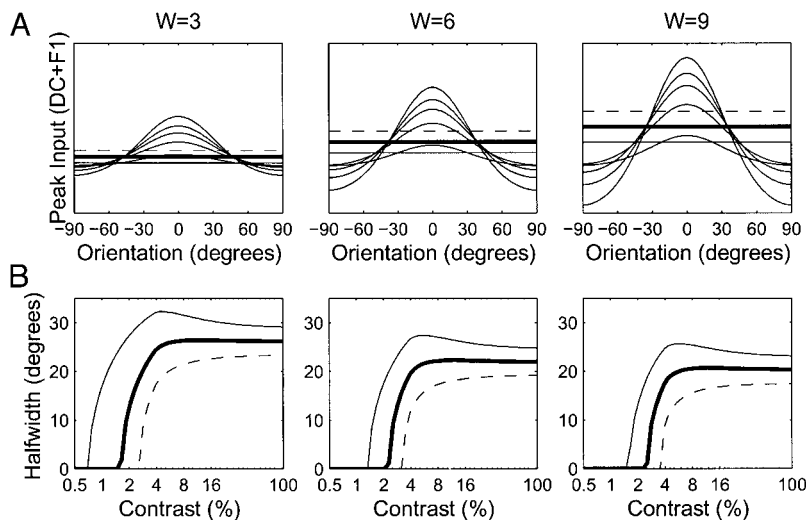


FIG. 4. Dependence of contrast invariance on the 2 model parameters, w and ψ^{eff} , using the linear rectified model of response to drifting sinusoidal gratings of Fig. 1. A: peak input as a function of orientation at 5 different contrasts (2, 4, 8, 16, and 64%) for 3 different levels of inhibition (left: $w = 3$; middle: $w = 6$; right: $w = 9$). All plots are shown with background level of input subtracted. Units chosen so that the modulation of the excitatory input for an optimal stimulus has unit magnitude [$F1_{\text{max}}(100)h(0) = 1$]. The 3 horizontal lines show 3 possible levels of effective threshold ψ^{eff} . The thick line represents the optimal threshold as defined by linear regression as in Fig. 3B. The thin and dashed lines deviate from this optimal by $\pm 0.1(1 + w)F1_{\text{max}}(100)$, i.e., $\pm 10\%$ of the total input modulation at 100% contrast. B: orientation tuning halfwidth as a function of contrast for the 3 levels of effective threshold shown in A. Peak inputs were calculated using Eq. 10 with $\phi_{\text{stim}} = 1$. Halfwidths were calculated from tuning curves constructed by integrating Eq. 11 over a complete cycle.

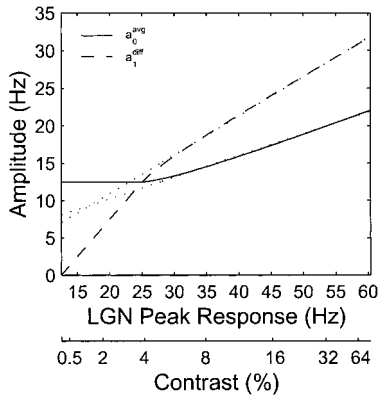


FIG. 5. a_0^{avg} and a_1^{diff} vs. peak amplitude of the ON/OFF-averaged component of LGN response $\{[ON_{peak}(C) + OFF_{peak}(C)]/2\}$, under the response model of Fig. 1. Contrasts corresponding to the given amplitudes are shown below plot. Dotted lines show best linear fit to 50 values of contrast spread evenly on a log scale from 5 to 100%. After LGN responses rectify (at contrasts above 5%), LGN response looks like a growing “hump” of activity and both the DC (a_0^{avg}) and F1 (a_1^{diff}) of the response grow linearly with the size of the hump.

orientation, and should result in a net inhibition having a similar contrast dependence as that of the modulated component of the total LGN input.

CONTRAST-INVARIANT ORIENTATION TUNING II: LOW-CONTRAST REGIME

Thus far we have shown that the threshold nonlinearity in the LGN, combined with strong push-pull inhibition, can be used to counteract the threshold-induced broadening of orientation tuning in cortical simple cells. Since the model relies in a crucial way on the rectification of LGN response, the model fails at low contrasts where LGN responses do not rectify. However, in this regime, where stimulus-induced LGN input is small and linear in contrast, the effects of noise on the spike threshold can yield contrast-invariant tuning.

We examine a model in which cortical spiking is governed by a rectified linear output function, and in which additive Gaussian noise is added to the stimulus-induced input (Amit and Tsodyks 1991; see also Abeles 1991). The output firing rate is then the mean rate averaged over the distribution of the noise. Adding such noise has the effect of “smoothing” the neuron’s input/output function (Fig. 6A) in the vicinity of threshold, allowing some responses even when the mean input is below threshold.³ In the regime of large inputs (far above threshold), the noise averages out and does not alter the linear-threshold input-output function.

Because the noise is able to boost the response to just-subthreshold inputs, it acts to broaden orientation tuning for low contrast stimuli. Thus comparing the peak input level (thin lines in Fig. 6B) with the resulting spike rate (thick lines), we find that the spike-rate tuning is significantly broader than the rectified input at contrasts below 5%. Plotting orientation tuning halfwidth versus contrast for a range of noise levels (Fig. 6C) demonstrates that this broadening counterbalances the narrowing of tuning seen for low contrast stimuli in the ab-

sence of noise and can lead to nearly contrast-invariant responses down to contrasts below 2% (dark line).

Power-law behavior

The mechanism underlying this noise-induced contrast invariance is that, for perithreshold inputs, the noise smoothing converts the rectified linear input/output function into a power-law input/output function (Miller and Troyer 2002)

$$r(C, \theta, \phi_{stim}) \cong [I_{LGN}(C, \theta, \phi_{stim}) - I_{LGN background}]^n$$

With a power-law input-output function, if the input I scales with the contrast, $I(C, \theta) = p(C)q(\theta)$, then so too does the output r

$$r(C, \theta) = [I(C, \theta)]^n = [p(C)q(\theta)]^n = [p(C)]^n [q(\theta)]^n = \hat{p}(C)\hat{q}(\theta) \quad (16)$$

Thus, given a power law, contrast-invariant input tuning implies contrast-invariant output tuning; this has previously been exploited in simple phenomenological models of cortical response (Albrecht and Geisler 1991; Heeger 1992).

For low contrasts, before LGN responses rectify, we expect the LGN input to scale with contrast. This can be seen from the fact that at these contrasts, the DC component does not change from background, so the input is given by a function of contrast times a function of orientation

$$I_{LGN}(C, \theta, \phi_{stim}) - I_{LGN background} = (1 + w)F1_{max}(C)h(\theta) \cos(\phi_{stim})$$

Thus, if noise creates a power-law input-output function at these low contrasts, then we expect contrast-invariant orientation tuning at these contrasts.

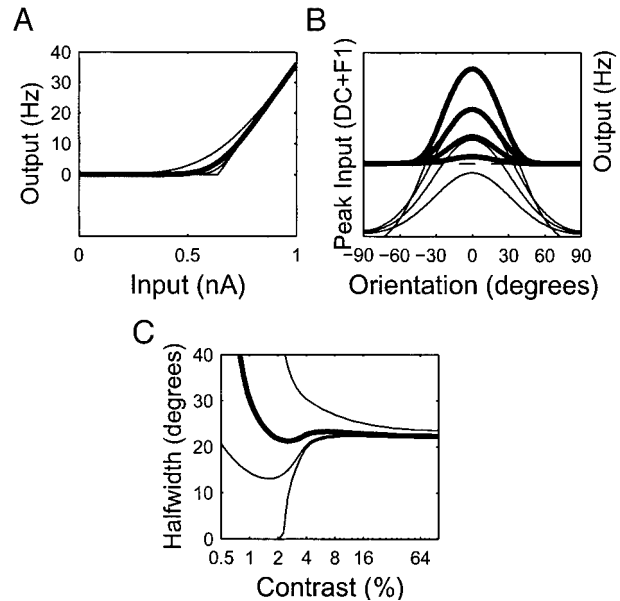


FIG. 6. Noise broadens tuning at low contrast. A: linear-rectified input/output smoothed by Gaussian noise. Input is expressed in units where $F1_{max}(100)h(0) = 1$. Increasing noise levels result in smoother functions (SD $\sigma = \{0, 0.05, 0.1, 0.2\}$). Note that the choice of output units is arbitrary; these can be rescaled without altering tuning by changing the gain g . B: peak input (thin lines) and spike rate (thick lines) obtained at 2, 3, 4, and 8% contrast ($\sigma = 0.1$; $w = 6$) under the LGN response model of Fig. 1. Horizontal line represents effective threshold ψ^{eff} on peak input scale, and rate of 0 Hz on output scale. C: orientation tuning halfwidth vs. contrast for the range of noise levels shown in A. $\sigma = 0.1$ (thick lines in A and C) gives contrast-invariant tuning to below 2% contrast.

³ Given the standard deviation of the noise σ , the spike threshold ψ , and the gain g , one can explicitly calculate the output firing rate as a function of the mean level of input I : $r = g(I - \psi)/2 [1 + \text{erf}((I - \psi)/\sigma\sqrt{2})] + g\sigma/\sqrt{2\pi} e^{-(I - \psi)^2/2\sigma^2}$, where erf is the error function, $\text{erf}(x) = 2/\sqrt{\pi} \int_0^x dy e^{-y^2}$.

Note that, for $n > 1$, the I^n response function sharpens output tuning relative to input F1 tuning, with larger n yielding greater sharpening. For higher contrasts where LGN responses rectify and the input-output function becomes linear, the output tuning is sharpened relative to input F1 tuning by the inhibition, with larger inhibition yielding greater sharpening. For tuning to be contrast invariant across the full range of contrasts, the sharpening induced by these two mechanisms must be equal.

DISCUSSION

There is widespread theoretical and experimental (Carandini and Ferster 2000; Gardner et al. 1999) agreement that the measured orientation tuning of simple cells requires relatively strong nonlinearities of cortical origin to sharpen the broadly tuned input from the LGN. The debate centers on *which* nonlinearities are best able to account for the range of experimental data. The threshold nonlinearity is perhaps the most obvious candidate (Carandini and Ferster 2000; Ferster 1987; Hubel and Wiesel 1962). However, in a naive threshold model, orientation tuning is expected to broaden with increasing contrast.

We have analyzed a very simple model of orientation tuning in which the threshold (or firing-rate rectification) nonlinearity was the only nonlinearity considered. We began with a careful analysis of the total LGN input to a cortical simple cell in response to a sinusoidal grating, finding 1) this input is well-approximated by a sinusoidal modulation about some mean level; 2) the amplitude of the modulation depends on both orientation and contrast, while that of the mean depends only on contrast; 3) the growth of the mean input with contrast is induced by the rectification of LGN responses; and 4) at contrasts where rectification of LGN responses is significant, both the mean level and the modulation amplitude grow roughly proportionally to the peak response of typical LGN cells.

Based on this analysis of the input, we then analyzed two routes to contrast-invariant orientation tuning. For a linear-threshold model of cortical spiking, we showed that contrast invariance requires that the mean and the modulation amplitude of the LGN input grow with identical shapes as a function of contrast, which is satisfied in the regime where rectification of LGN responses is significant. Intuitively, strong push-pull inhibition converts the mean input into a net inhibitory input, which eliminates the contrast-dependent broadening of tuning expected from a simple threshold model and yields sharp, contrast-invariant tuning. At very low contrasts, LGN rectification does not occur. However, neuronal noise can smooth the linear-threshold response function, yielding a power function to a good approximation. As a result, the model again yields sharp, contrast-invariant tuning (Miller and Troyer 2002). If the sharpening of tuning induced by the approximate power-law nonlinearity at lower contrasts matches the sharpening induced by inhibition and spike threshold at higher contrasts, this simple model can account for contrast-invariant orientation tuning over the full range of contrasts.

Parameter dependence

Our analysis suggests that the contrast invariance of orientation tuning depends on correct choice of parameters in two

respects. First, the threshold ψ^{eff} must be chosen to satisfy the analytic condition for contrast invariance in the high-contrast regime. However, we showed here in numerical simulations that the resulting contrast invariance of tuning, as measured by the half-width at half height of the orientation tuning curve, is relatively insensitive to the exact placement of spike threshold. Second, parameter tuning seems required to match tuning width at very low contrasts, where sharpening of tuning is determined by the exponent in the power-law response function, to tuning width at higher contrasts, where sharpening of tuning is determined by the strength of inhibition.

The analysis of the simple model studied here may underestimate the robustness with which dominant antiphase inhibition and neural noise achieve contrast-invariant tuning. In our previous simulations of a more biophysically realistic network model, we did not tune threshold or noise levels,⁴ yet contrast-invariant tuning resulted down to very low contrasts and across a range of inhibition strengths (see Fig. 5A of Troyer et al. 1998; orientation tuning broadened slightly at the lowest contrast studied, 2.5%, but such broadening at very low contrasts is also suggested by the experimental data, Skottun et al. 1987).

Alternative models

The two nonlinear mechanisms considered here—1) linear LGN input and a nonlinear (power-law) cortical transfer function, and 2) nonlinear LGN input (rectified, so that the mean grows with contrast), strong push-pull inhibition, and a linear-threshold cortical transfer function—can be contrasted with a third class of nonlinear models. These models rely on the interaction between the threshold nonlinearity and strong center-surround connectivity within the cortex to achieve contrast-invariant tuning (Ben-Yishai et al. 1995; Somers et al. 1995). These models use recurrent dynamics that result in an “activity bubble” of cortical response, whose shape is determined by the pattern of intracortical connections in a manner largely independent of the pattern of LGN input. The shape of this activity bubble in turn determines the shape of the orientation tuning curve. As a result, orientation tuning is invariant to changes in the pattern of LGN input, and in particular is invariant to changes in stimulus contrast. However, these models are inconsistent with a number of experimental results demonstrating basic linear elements of simple cell receptive fields. In particular, there is a correspondence between the linear component of response as measured with spatially localized stimuli and with drifting sinusoidal gratings (Gardner et al. 1999; Jones and Palmer 1987a; Lampl et al. 2001; Movshon et al. 1978). Moreover, orientation tuning is not independent of all input parameters. Rather, tuning depends on the spatial frequency of oriented gratings (Hammond and Pomfrett 1990; Vidyasagar and Sigüenza 1985; Webster and De Valois 1985) and the length of oriented bars (Vogels and Orban 1990) in the manner predicted by the present model (Troyer et al. 1998): stimuli that evoke narrower tuning of the LGN input modulation evoke narrower tuning of the cortical spike response.

⁴ Spike threshold was set to -52.5 mV, and then sufficient nonspecific background excitatory conductances were injected to produce low, physiological levels of spontaneous spiking activity in excitatory cells at the “default” level of inhibition. This amounts to setting threshold in units of the noise. Neither threshold nor the amount of injected background conductance were varied as the strength of inhibition was changed.

A recent model of monkey layer 4 (McLaughlin et al. 2000; Wielaard et al. 2001) also relies on strong feed-forward inhibition to cancel the nonlinear component of LGN input, but assumes that this inhibition has no phase specificity. This accords with the lack of phase specificity of transient inhibitory responses reported by some workers (Borg-Graham et al. 1998) but not by others (Ferster 1988; Hirsch et al. 1998). Phase-nonspecific inhibition would contribute an inhibitory DC component, but no F1 component, to the response to a periodic grating. Thus the effect of including such inhibition in our model would be to replace the factor $(1 - w)$ multiplying $DC(C)$ in Eq. 10 by $(1 - w - w_{\text{non}})$, where w still represents the phase-specific component of inhibition and w_{non} represents the phase-nonspecific component. This in turn would cause the condition for contrast-invariant tuning, Eq. 14, to be modified simply by replacing $(w - 1)$ with $(w + w_{\text{non}} - 1)$. Thus phase-nonspecific inhibition is equally as effective as phase-specific inhibition in achieving contrast-invariant tuning. The main difference between the two is that phase-specific inhibition enhances the response to a preferred stimulus (it adds to the F1 while subtracting from the DC), while phase-nonspecific inhibition equally suppresses responses to a preferred or nonpreferred stimulus (it does not add to the F1 while subtracting from the DC). Thus substituting phase-nonspecific for phase-specific inhibition will reduce responses and sharpen orientation tuning by rendering more orientations subthreshold.

A key prediction of our model is that at least a subset of layer 4 inhibitory cells should respond in a contrast-dependent manner to all orientations (Troyer et al. 1998). Inhibition from these cells is necessary to prevent the untuned component of the LGN input from driving spiking in tuned simple cells at orientations far from the cell's preferred orientation. Hirsch et al. (2000) recently reported two classes of inhibitory cells in cat V1 layer 4: simple cells that appeared to have good orientation tuning and complex cells that were essentially untuned for orientation. Such complex cells could provide the contrast-dependent untuned inhibition required by our formulation, although in a different form than used in our model. The inhibition from these complex cells would contribute to the DC but not to the F1, just as phase-nonspecific inhibition would. The simple inhibitory cells would provide phase-specific, push-pull inhibition at orientations around the preferred but would not spike far from the preferred orientation, presumably because they are inhibited by the complex cells in a manner similar to excitatory simple cells.

Voltage tuning versus input tuning

Anderson et al. (2000b) have published experimental data indicating that the full range of contrast responses lies in a noise-dominated regime. They found that voltage noise was large, e.g., rms 5 mV, comparable with the voltage DC and F1 at high contrast, which were each 5–10 mV. They also found that the mean and modulation of the voltage response each had similar orientation tuning and that the tuning of each simply scaled with contrast. They showed that this, the large noise, and a linear-threshold model for converting voltage responses to spiking responses could yield contrast-invariant spiking responses, much as in our low-contrast regime. At first glance it might appear that this makes our analysis of the high-contrast regime irrelevant, because the noise-smoothed part of the in-

put/output curve applies over the full range of contrasts. However, the model proposed by Anderson et al. begins with the observed voltage responses; it does not address the mechanisms by which the LGN input drive is converted into the observed tuning and contrast scaling of the voltage.

In the model analyzed here, spiking output is assumed to be a rectified linear function of a cell's synaptic input, smoothed by noise. The intermediate step of conversion of synaptic input into membrane voltage is not addressed. In particular, the model does not include the nonlinearity contributed by synaptic reversal potentials. This nonlinearity should not have much effect on spiking responses, since deviations from linear behavior are small at voltages near and above threshold (Holt and Koch 1997). However, near the inhibitory reversal potential, inhibitory drive is significantly reduced, but excitatory drive is relatively unchanged. Thus a linear model would systematically overestimate the degree of membrane hyperpolarization for subthreshold ranges of voltage.

Nonetheless, our analysis of the LGN input has interesting implications for understanding the results of Anderson et al. (2000b). We focus on two significant results. First, Anderson et al. (2000b) found little stimulus-induced voltage change from rest at any contrast in response to stimuli of the null orientation (the orientation orthogonal to the preferred), a result also seen by Carandini and Ferster (2000). Our analysis suggests that null-oriented stimuli should evoke significant LGN excitation that grows with contrast.⁵ To prevent significant depolarization from rest, this excitation must be balanced by an equal amount of inhibitory current. However, equivalence of excitatory and inhibitory currents near rest translates into a dominance of inhibition for membrane potentials near threshold. Thus the lack of depolarization to stimuli at the null orientation suggests that the mean input in response to these stimuli is inhibition dominated, as required by our model.

Second, the mean level of membrane depolarization (the voltage DC) in simple cells is tuned for orientation and has tuning similar to that of the voltage modulation (the voltage F1) (Anderson et al. 2000b; Carandini and Ferster 2000). The orientation tuning of the mean voltage response may be induced by two nonlinearities interacting with the voltage modulation. First, the inhibitory reversal potential prevents much hyperpolarization from rest, but does not limit depolarizations, so that voltage modulations will be primarily depolarizing from rest. Second, the tuned spiking response driven by the modulation of the LGN input will be amplified by input from other cortical cells in the same or nearby orientation columns that are also driven to spike (Anderson et al. 2000a; Douglas et al. 1995; Ferster 1986; Troyer et al. 1998). The net depolarization from each of these nonlinearities should cause the voltage DC to inherit orientation tuning similar to that of the voltage F1.

Conclusion

A number of factors can contribute to the orientation tuning of voltage and spiking in cortical simple cells. These include

⁵ Yet another complication is that the mean LGN input may be suppressed by frequency-dependent synaptic depression at lower temporal frequencies, e.g., 2 Hz (Krukowski 2000). However, at higher temporal frequencies, e.g., 8 Hz, the effects of the untuned mean LGN input should be strong. Anderson et al. (2000b) and Carandini and Ferster (2000) studied only lower temporal frequency stimuli.

nonlinearities in the LGN input, the threshold nonlinearity and its possible smoothing by noise, antiphase inhibition, phase-nonspecific or orientation-untuned inhibition, reversal potential nonlinearities, and the input from other cortical excitatory cells. We have addressed the first three factors in a model that is simple enough to allow analysis, and that emphasizes the role played by contrast-dependent nonlinearities in the LGN. The results of Anderson et al. (2000b) suggest that noise smoothing plays a key role in the contrast invariance of orientation tuning over the full range of contrasts, which differs from the model presented here. Nonetheless, our analysis of the LGN suggests the need for dominant feed-forward inhibition that eliminates response to the DC component of the LGN input, while also pointing out a route to contrast-invariant tuning for stimuli that might push a cell beyond the noise-smoothed regime. More generally, our analysis suggests that decomposing simple cell input into ON/OFF-averaged and ON/OFF-specific components may be a useful step toward a more complete understanding of orientation tuning in layer 4.

We gratefully acknowledge support by National Eye Institute Grant EY-11001 (K. D. Miller) and the Howard Hughes Medical Institute predoctoral fellowship program (A. E. Krukowski).

REFERENCES

- ABELES M. *Corticomics: Neural Circuits of the Cerebral Cortex*. Cambridge, MA: Cambridge Univ. Press, 1991.
- ALBRECHT DG AND GEISLER WS. Motion selectivity and the contrast-response function of simple cells in the visual cortex. *Vis Neurosci* 7: 531–546, 1991.
- AMIT DJ AND TSODYKS MV. Quantitative study of attractor neural network retrieving at low spike rates: I. substrate-spikes, rates and neuronal gain. *Network* 2: 259–273, 1991.
- ANDERSON JS, CARANDINI M, AND FERSTER D. Orientation tuning of input conductance, excitation, and inhibition in cat primary visual cortex. *J Neurophysiol* 84: 909–926, 2000a.
- ANDERSON JS, LAMPL I, GILLESPIE D, AND FERSTER D. The contribution of noise to contrast invariance of orientation tuning in cat visual cortex. *Science* 290: 1968–1972, 2000b.
- BEN-YISHAI R, BAR-OR RL, and Sompolinsky H. Theory of orientation tuning in visual cortex. *Proc Natl Acad Sci USA* 92: 3844–3848, 1995.
- BORG-GRAHAM LJ, MONIER C, AND FRÉGNAC Y. Visual input evokes transient and strong shunting inhibition in visual cortical neurons. *Nature* 393: 369–373, 1998.
- BRUMBERG JC, PINTO DJ, AND SIMONS DJ. Spatial gradients and inhibitory summation in the rat whisker barrel system. *J Neurophysiol* 76: 130–140, 1996.
- BULLIER J AND HENRY GH. Laminar distribution of first-order neurons and afferent terminals in cat striate cortex. *J Neurophysiol* 42: 1271–1281, 1979.
- CARANDINI M AND FERSTER D. Membrane potential and firing rate in cat primary visual cortex. *J Neurosci* 20: 470–484, 2000.
- CHENG H, CHINO YM, SMITH EL, HAMAMOTO J, YOSHIDA K. Transfer characteristics of lateral geniculate nucleus X neurons in the cat: effects of spatial frequency and contrast. *J Neurophysiol* 74: 2548–2557, 1995.
- DOUGLAS RJ, KOCH C, MAHOWALD M, MARTIN KA, AND SUAREZ HH. Recurrent excitation in neocortical circuits. *Science* 269: 981–985, 1995.
- FERSTER D. Orientation selectivity of synaptic potentials in neurons of cat primary visual cortex. *J Neurosci* 6: 1284–1301, 1986.
- FERSTER D. Origin of orientation-selective EPSPs in simple cells of cat visual cortex. *J Neurosci* 7: 1780–1791, 1987.
- FERSTER D. Spatially opponent excitation and inhibition in simple cells of the cat visual cortex. *J Neurosci* 8: 1172–1180, 1988.
- FERSTER D AND LINDSTRÖM S. An intracellular analysis of geniculocortical connectivity in area 17 of the cat. *J Physiol (Lond)* 342: 181–215, 1983.
- FERSTER D AND MILLER KD. Neural mechanisms of orientation selectivity in the visual cortex. *Annu Rev Neurosci* 23: 441–471, 2000.
- GARDNER JL, ANZAI A, OHZAWA I, AND FREEMAN RD. Linear and nonlinear contributions to orientation tuning of simple cells in the cat's striate cortex. *Vis Neurosci* 16: 1115–1121, 1999.
- GILBERT CD. Laminar differences in receptive field properties of cells in cat primary visual cortex. *J Physiol (Lond)* 268: 391–421, 1977.
- HAMMOND P AND POMFRETT CJ. Influence of spatial frequency on tuning and bias for orientation and direction in the cat's striate cortex. *Vision Res* 30: 359–369, 1990.
- HEEGER DJ. Half-squaring in responses of cat striate cells. *Vis Neurosci* 9: 427–443, 1992.
- HIRSCH JA, ALONSO J-M, PILLAI C, AND PIERRE C. Simple and complex inhibitory cells in layer 4 of cat visual cortex. *Soc Neurosci Abstr* 26: 1083, 2000.
- HIRSCH JA, ALONSO J-M, REID RC, AND MARTINEZ LM. Synaptic integration in striate cortical simple cells. *J Neurosci* 18: 9517–9528, 1998.
- HOLT GR AND KOCH C. Shunting inhibition does not have a divisive effect on firing rates. *Neural Comput* 9: 1001–1013, 1997.
- HUBEL DH AND WIESEL TN. Receptive fields, binocular interaction and functional architecture in the cat's visual cortex. *J Physiol (Lond)* 160: 106–154, 1962.
- JONES JP AND PALMER LA. An evaluation of the two-dimensional Gabor filter model of simple receptive fields in cat striate cortex. *J Neurophysiol* 58: 1233–1258, 1987a.
- JONES JP AND PALMER LA. The two-dimensional spatial structure of simple receptive fields in cat striate cortex. *J Neurophysiol* 58: 1187–1211, 1987b.
- KRUKOWSKI AE. *A Model of Cat Primary Visual Cortex and Its Thalamic Input* (PhD thesis). San Francisco, CA: Univ. of California, 2000.
- LAMPL I, ANDERSON J, GILLESPIE D, AND FERSTER D. Prediction of orientation selectivity from receptive field architecture in simple cells of cat visual cortex. *Neuron* 30: 263–274, 2001.
- MCLAUGHLIN D, SHAPLEY R, SHELLEY M, AND WIELAARD DJ. A neuronal network model of macaque primary visual cortex (V1): orientation selectivity and dynamics in the input layer 4 α . *Proc Natl Acad Sci USA* 97: 8087–8092, 2000.
- MILLER KD AND TROYER TW. Neural noise can explain expansive, power-law nonlinearities in neural response functions. *J Neurophysiol* 87: 653–659, 2002.
- MOVSHON JA, THOMPSON ID, AND TOLHURST DJ. Spatial summation in the receptive fields of simple cells in the cat's striate cortex. *J Physiol (Lond)* 283: 53–77, 1978.
- REID RC AND ALONSO JM. Specificity of monosynaptic connections from thalamus to visual cortex. *Nature* 378: 281–284, 1995.
- SAUL AB AND HUMPHREY AL. Spatial and temporal response properties of lagged and nonlagged cells in cat lateral geniculate nucleus. *J Neurophysiol* 64: 206–224, 1990.
- SCLAR G AND FREEMAN RD. Orientation selectivity in the cat's striate cortex is invariant with stimulus contrast. *Exp Brain Res* 46: 457–461, 1982.
- SKOTTUN BC, BRADLEY A, SCLAR G, OHZAWA I, AND FREEMAN RD. The effects of contrast on visual orientation and spatial frequency discrimination: a comparison of single cells and behavior. *J Neurophysiol* 57: 773–786, 1987.
- SOMERS D, NELSON SB, AND SUR M. An emergent model of orientation selectivity in cat visual cortical simple cells. *J Neurosci* 15: 5448–5465, 1995.
- SWADLOW HA. Neocortical efferent neurons with very slowly conducting axons: strategies for reliable antidromic identification. *J Neurosci Methods* 79: 131–141, 1998.
- TROYER TW, KRUKOWSKI AE, AND MILLER KD. Contrast-invariant orientation tuning in cat visual cortex: an analysis. *Soc Neurosci Abstr* 25: 1933, 1999.
- TROYER TW, KRUKOWSKI AE, PRIEBE NJ, AND MILLER KD. Contrast-invariant orientation tuning in cat visual cortex: feedforward tuning and correlation-based intracortical connectivity. *J Neurosci* 18: 5908–5927, 1998.
- VIDYASAGAR TR AND SIGÜENZA JA. Relationship between orientation tuning and spatial frequency in neurons of cat area 17. *Exp Brain Res* 57: 628–631, 1985.
- VOGELS R AND ORBAN GA. How well do response changes of striate neurons signal differences in orientation: a study in the discriminating monkey. *J Neurosci* 10: 3543–3558, 1990.
- WEBSTER MA AND DE VALOIS RL. Relationship between spatial-frequency and orientation tuning of striate-cortex cells. *J Opt Soc Am A* 2: 1124–1132, 1985.
- WIELAARD DJ, SHELLEY M, McLaughlin D, and Shapley R. How simple cells are made in a nonlinear network model of the visual cortex. *J Neurosci* 21: 5203–5211, 2001.
- WOLFE J AND PALMER LA. Temporal diversity in the lateral geniculate nucleus of cat. *Vis Neurosci* 15: 653–675, 1998.